Schweizer Jugend forscht 2020

Sinking Bubbles

Ophélie Rivière*

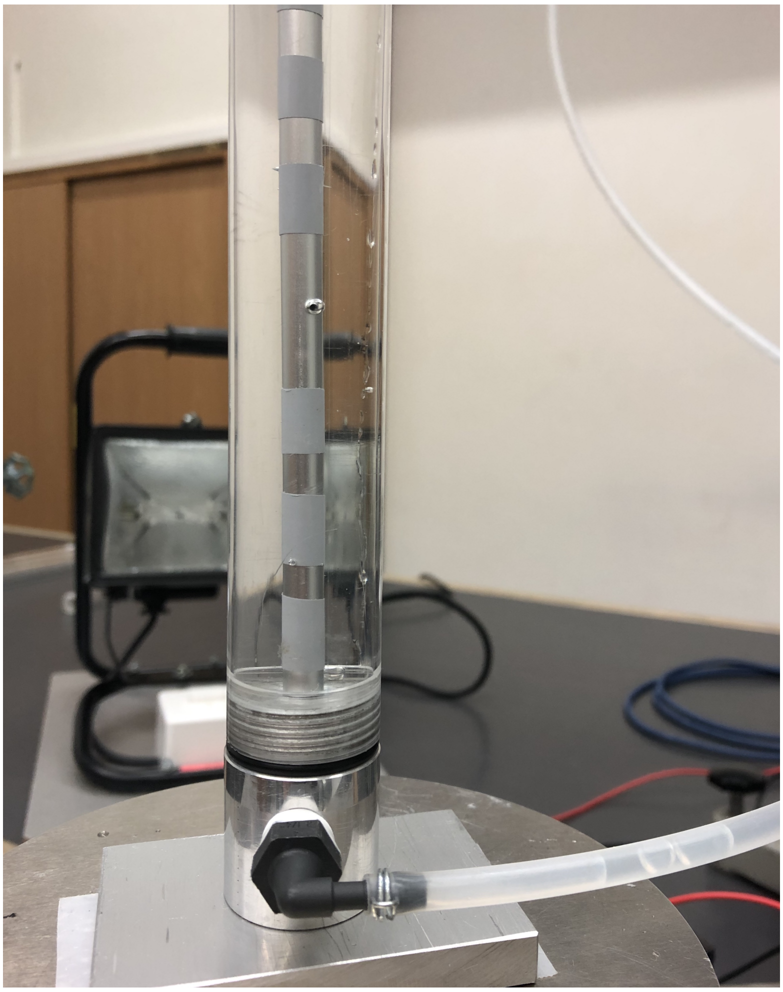

*MNG Rämibühl CH-8001 Zürich, Switzerland.

Abstract

This paper aims to explain the motion of sinking bubbles in a vertically oscillating liquid by testing the existing theory on the subject. The conditions under which the formulas of earlier studies accurately describe the motion of sinking bubbles have been determined experimentally. These experiments brought light to some shortcomings in the previously published results. In this paper, I confirm for the first time that the static theory applies and define the regime in which the equation of motion is applicable. In addition, I provide an alternate equation of motion that can be used under specific conditions.

Contents

I Introduction

In 2019, I participated in the Swiss Young Physicists Tournament (SYPT). Out of the 17 problems proposed, problem number 16, sinking bubbles, immediately caught my interest. The task was "When a container of liquid (e.g. water) oscillates vertically, it is possible that bubbles in the liquid move downwards instead of rising. Investigate the phenomenon."

I was particularly curious about this phenomenon because it is very much counterintuitive. A bubble of air can sink in water even though the densities have a difference of three orders of magnitude. What stroke me after studying the publications about this problem, is that none of them included experiments to confirm the theory. In a first paper [3], Elizer Rubin proposes a model that looks at the state of the vibrating bubble, whether it is rising, sinking or remaining at the same depth. In other publications for example [2, 7], one can find an equation of motion that aims to describe the bubble's position at any point in time. The results of the research in that topic is applicable in the development and optimisation of some relevant technologies like the floatation process.

In this paper I provide results of experiments of sinking air bubbles in both water and oil varying the following parameters: depth, amplitude, frequency and the liquid's density and viscosity. Moreover, some shortcomings of previous publications are highlighted and a variation of the theory one can use in a defined system is proposed. Lastly, for both equations of motion, the conditions in which they accurately describe the behaviour of sinking bubbles are elaborated.

II Theory

Usually, bubbles in a liquid rise due to the density difference between the liquid and gas. A bubble in a liquid will experience a pressure according to its position. Hence, it will experience a pressure gradient. If one starts oscillating the column of liquid, the pressure changes will also be dependent on the oscillator's acceleration. When such an acceleration leads to a pressure inversion, e.g. if the liquid is accelerated downwards by more than the earth's acceleration, the bubbles will start moving downwards, as they always go where the pressure is at the lowest.

The vertical oscillation is harmonic. This means the acceleration and so the buoyancy force acting on the bubble are time dependent. At a fixed depth you observe fluctuations in the pressure and the bubbles undergo a driven oscillation (see Figure 1).

In order for the bubbles to sink, the drive and the response must be in phase. To make sure this holds true, I calculated the Minneart Resonance of the bubble [5]: $\omega_R = 3.3$ kHz.

For frequencies below 100 Hz, one can expect good results. In an upwards acceleration, the water at the bottom of the tube is compressed and the bubble experiences a higher pressure whereas during a downwards acceleration, when the oscillator's acceleration is above the earth's acceleration, the water is in a falling motion, which leads to an underpressure at the bottom of the tube and so the pressure exerted on the bubble decreases.

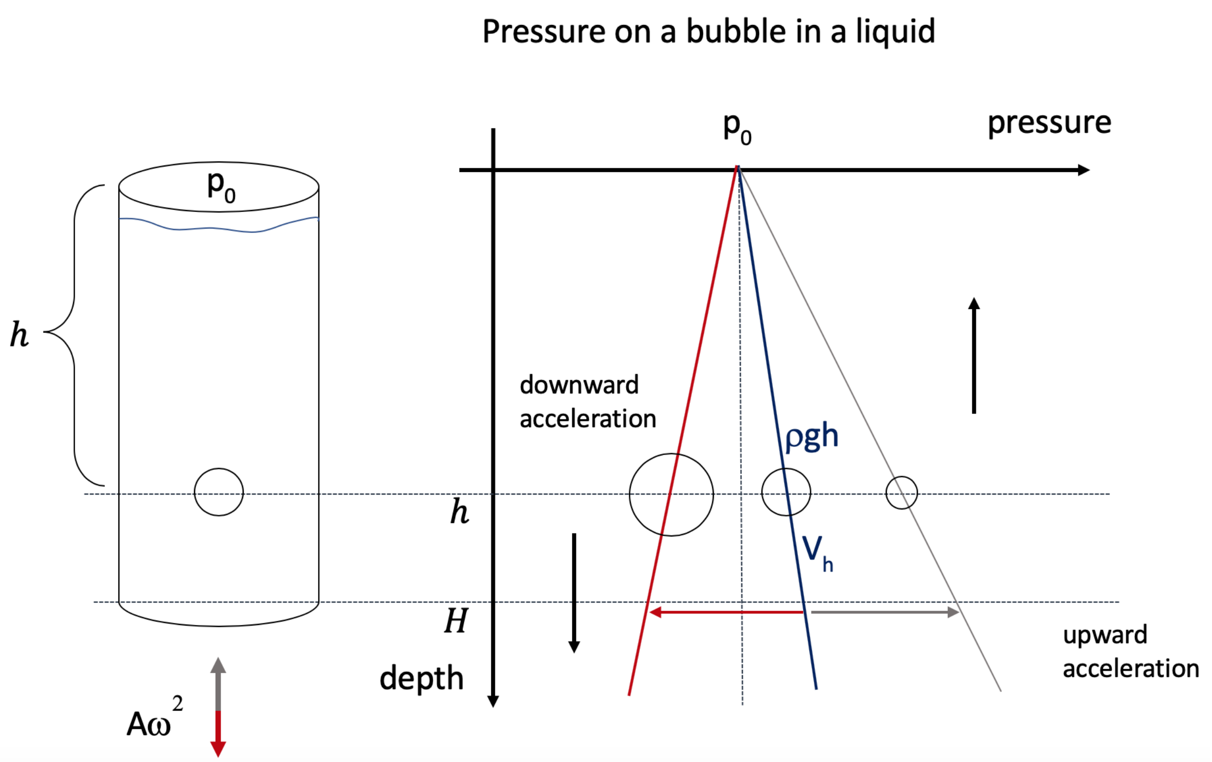

Figure 1: The blue function shows the dependency of the pressure as a function of the depth in a none vibrating liquid. In this case the formula $p = \rho g h$ is applicable. The grey and red functions show the same dependency when the liquid is oscillating in a vertical direction. In those cases, the pressure, given by the non vibrating case for any depth h, will be decreased for a downward acceleration or increased for an acceleration in opposite direction.

II.1 The Static Case

Bubbles in a vertically oscillating liquid of density ρ experience a change in pressure p, which implies a change in volume V. If the average buoyancy force over one period equals to zero, the bubbles stay at the same depth. In case the result is positive, the bubbles are rising and they are sinking if the value is negative.

The pressure on the bubble can be written as:

$$p = p_0 + \rho(g + A\omega^2 sin(\omega t))h = p_0 + \rho g h + \rho A\omega^2 sin(\omega t)h \tag{II.1}$$

Since we look at the bubble at constant depth we can use

$$\Delta p(t) = \rho A\omega^2 sin(\omega t)h \quad . \tag{II.2}$$

The buoyancy force can be expressed as:

$$F = \rho V(t)a(t)$$

$$F = \rho(V_h + \Delta V(t))(g + A\omega^2 sin(\omega t)) \tag{II.3}$$

V_h is the volume of the bubble at depth h in the stagnant liquid and ΔV the change in volume during the oscillation. It is defined as:

$$\Delta V(t) = -\beta V_h \Delta p(t) \tag{II.4}$$

where the compressibility factor β is equal to

$$\beta = \frac{1}{\gamma p_0} \quad . \tag{II.5}$$

γ is the polytropic exponent. $\gamma = 1$ if the compressibility is isothermal and if it is adiabatic $\gamma = 1.4$. The compressibility is assumed to be adiabatic since the oscillation happens so quickly that an exchange of heat is highly improbable.

Entering the expressions for beta and $\Delta p(t)$ in the equation of the change in volume one gets

$$\Delta V(t) = -\frac{1}{\gamma p_0} V_h \rho A\omega^2 sin(\omega t)h \quad . \tag{II.6}$$

If I insert the expression for ΔV in the equation II.4 and I get:

$$F = \rho(V_h - \frac{1}{\gamma p_0} V_h \rho A\omega^2 sin(\omega t)h)(g + A\omega^2 sin(\omega t)) \quad . \tag{II.7}$$

To get the average buoyancy force, I take the integral of this equation over one period and divide it by the period.

$$
\begin{aligned}
< F > &= \frac{1}{T}\int_0^T \rho(V_h - \frac{1}{\gamma p_0}V_h\rho A\omega^2 sin(\omega t)h)(g + A\omega^2 sin(\omega t))dt \\
&= \frac{1}{T}\int_0^T \rho V_h g + \rho V_h A\omega^2 sin(\omega t) - \frac{\rho^2}{\gamma p_0}V_h A\omega^2 sin(\omega t)gh \\
&\quad -\frac{\rho^2}{\gamma p_0}V_h A^2\omega^4 sin^2(\omega t)hdt \qquad \text{(II.8)} \\
&= \rho V_h g - \frac{\rho}{2\gamma p_0}V_h\rho A^2\omega^4 h \\
&= \rho V_h g\left(1 - \frac{\rho A^2\omega^4 h}{2\gamma g p_0}\right)
\end{aligned}
$$

You can set the average buoyancy force equal to zero and obtain the conditions for a static bubble.

$$
\begin{aligned}
1 &= \frac{\rho A^2\omega^4 h}{2\gamma g p_0} \\
A\omega^2 &= \sqrt{\frac{2\gamma g p_0}{\rho h}} \qquad \text{(II.9)}
\end{aligned}
$$

Equation II.9 was found in reference [3] and is validated in section IV on Figures 6 and 7.

II.2 Dynamics

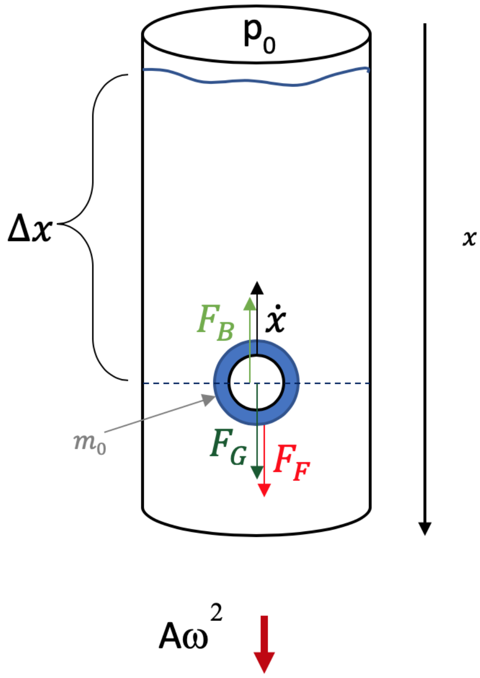

Figure 2: This sketch shows the forces acting on a rising bubbles in a system that is being accelerated downwards. Please note that the x-axis is pointing downwards and represents the depth.

In literature [2, 7] you can find the following equation that is meant to describe the dynamic motion of a sinking bubble.

$$(m + m_0)\ddot{x} + m_0\dot{x} = -\frac{1}{2}C\rho A_B\ddot{x}^2 + (m - \rho V_b)(A\omega^2 sin(\omega t) + g) \tag{II.10}$$

It shows a correct qualitative behaviour. I however aim for a quantitative evaluation to measure the reliability of equation II.10 (see section V.1).

Figure 2 shows the forces used in equation II.10,

$$F_F = \frac{1}{2}C\rho A_B\ddot{x}^2 \tag{II.11}$$

$$F_G = m_B(A\omega^2 sin(\omega t) + g)$$

$$F_B = \rho V_b(A\omega^2 sin(\omega t) + g)$$

as well as a representation of the added mass, m_0, the mass of the water which oscillates along with the bubble,

$$m_0 = \frac{2}{3}\,\pi\,\rho\,r_B^3 \tag{II.12}$$

where $\frac{2}{3}$ is the coefficient of added mass for a sphere [1]. This coefficient seems to be an insufficient approximation. While the column oscillates, the bubble's shape does not maintain its round form, which means one can not consider it as a sphere any longer (see Figure 3).

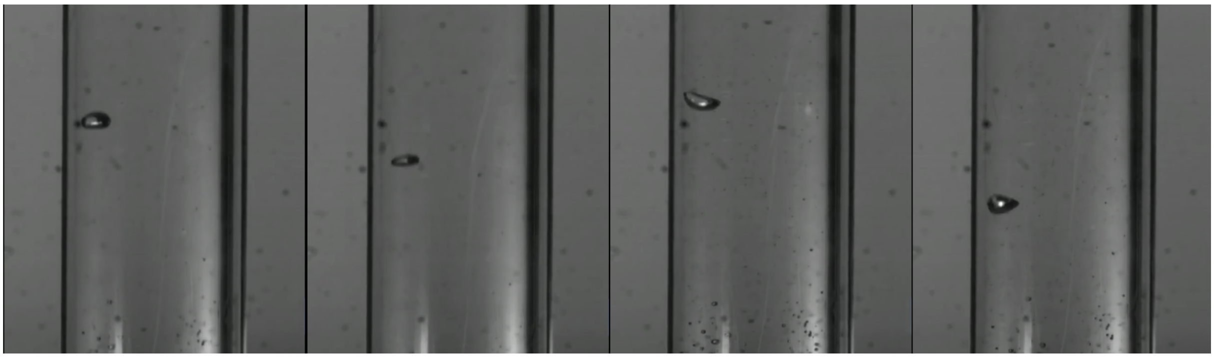

Figure 3: Shape of a sinking bubble of large radius in a vertical oscillation over time.

The capillary length, λ_{cap}, is a scaling factor relating gravity and surface tension. The ratio of the radius of the bubble to the capillary length, indicates how close the bubble's shape will be to a sphere. If

$$\frac{r}{\lambda_{cap}} = \sqrt{\frac{\rho g r^2}{\sigma}} = 0$$

the bubble is spherical. The higher the result of the equation the more significant the deviation away from the sphere gets [4]. Calculations of the capillary length are available in the appendix (see section B).

As the capillary length is constant for bubbles of air in water, the smaller the radius of the bubble the more spherical it will be. Which means one can try a workaround the problem by choosing the bubble's radius as small as possible. The change in volume is in such a case less important and there is a better chance for equation II.12 to be accurate. A smaller bubble implies a reduced velocity and both together speak for a low Reynolds number (see section II.3). A further way to lower the number is to change the fluid to a more viscous one e.g. sunflower oil. If equation II.10 gives a relatively good simulation for water under certain conditions, changes will be made in the theory for the case in oil.

The flow is always laminar. However, Stokes' law can and must be applied for lower Reynolds numbers. Consequently, I adapt the equation of the friction force.

$$F_F = 6\pi\eta\dot{x}r$$

Furthermore, due to smaller accelerations, the oscillating mass around the bubble get's much smaller and can therefore be neglected. The resultant force is then written as follows:

$$\frac{d}{dt}m_B\dot{x} = -6\pi\eta\dot{x}r + (m_B - \rho V_b)(A\omega^2 sin(\omega t) + g) \quad . \tag{II.13}$$

II.3 The Reynolds Number

The Reynolds number of a motion is a number describing the flow of this motion. It is the ratio between the inertia and the friction force. Hence, this number is dimensionless. The value of the Reynolds number can be found by applying the following equation

$$Re = \frac{vd\rho}{\eta} \tag{II.14}$$

and is dependent on v the velocity of the bubble, d its diameter, η the liquid's viscosity and ρ the corresponding liquid density.

The Reynolds number permits to determine what equation shall be used for the friction force. For $Re \leq 2$ Stokes' law is very accurate. It is believed that Stokes' law can be applied for values of the Reynolds number lower than 4. For larger Reynolds numbers, the more general Equation II.11 can be used, where C depends a priori on the Reynolds number, Re. In a very large range C decreases with increasing Reynolds number; in the range between approximately 1000 to 500000, the value of C is constant [6].

III Materials and Methods

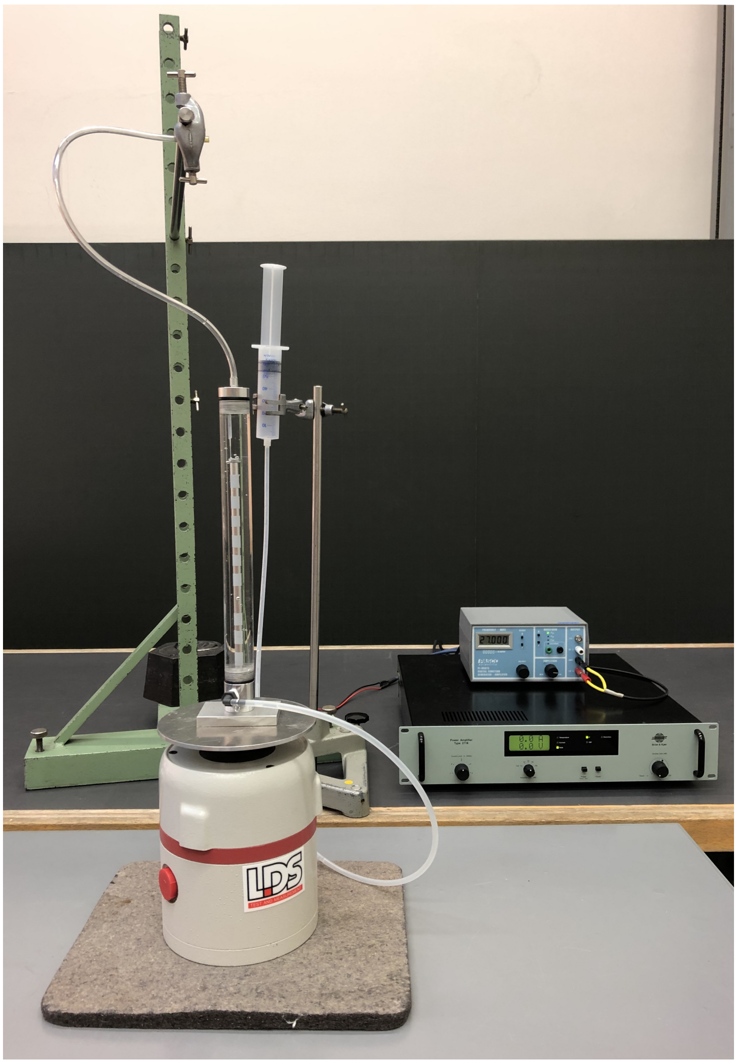

Figure 4: Picture of the set up. For my experiments I used an oscillator (LDS Shaker V406) that oscillates vertically with a frequency determined through a signal generator and amplitude set by the amplifier. Furthermore, I used tubes of different lengths (28.4 cm$\leq$ l $\leq$ 57.9 cm) at the bottom of which I could press air through a hose with a syringe. To keep an ambient pressure on top of the tube a hose is attached to the cap and lets the air out. In the main tube one can see a smaller tube (see Figure 5), it permits the beginning depth to be smaller than the maximal depth which makes it easier to distinguish whether the bubbles are sinking, remaining at the same depth or rising.

The first series of experiments consisted of measuring the critical amplitude. That means the amplitude at which bubbles would be in a static motion for a given frequency and bubble depth. To do so I would install the set up as shown in Figure 4 and start accelerating the shaker by going up with the amplitude. I would then press the syringe to let air in the column and see whether the bubbles would sink or rise. Were they rising, I would increase the amplitude and start again. If the bubbles started to sink I would decrease the amplitude slowly and check again whether the bubbles were in a sinking, static or rising motion. By increasing and decreasing the amplitude I could go as close as possible to the critical value. When it was found I would film the oscillator with a high speed camera (500 frames per second) to be able to, later on, track the amplitude at which bubbles are in a static motion and compile a diagram out of the measured points.

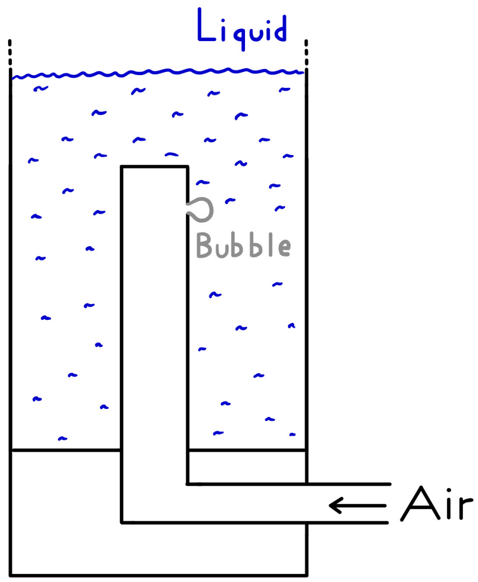

Figure 5: Sketch of the entry of air with the use of the inner tube. The sketch shows the cross section of the bottom of the main tube.

The second type of experiments that I conducted was made to follow the development of a bubble in the vibrating column over time. For this series of experiments the inner tube (see Figure 4) was removed to assure a clearer view on the bubble. The first step was to choose a fixed depth and frequency and then approximately decide with what amplitude I wanted the shaker to oscillate. Some air would then be pressed at the lowest point of the tube. I would choose an isolated bubble, to capture it's behaviour over time. This was done with the high speed camera at 500 frames per second. Later on, I would track the bubble's motion and measure its diameter to compare the experimental results to the theory.

IV The Static Case

IV.1 Experimental Results

Please note that all theoretical values are derived from section II. The following diagrams are based on equation II.9 and all error bars are statistical errors.

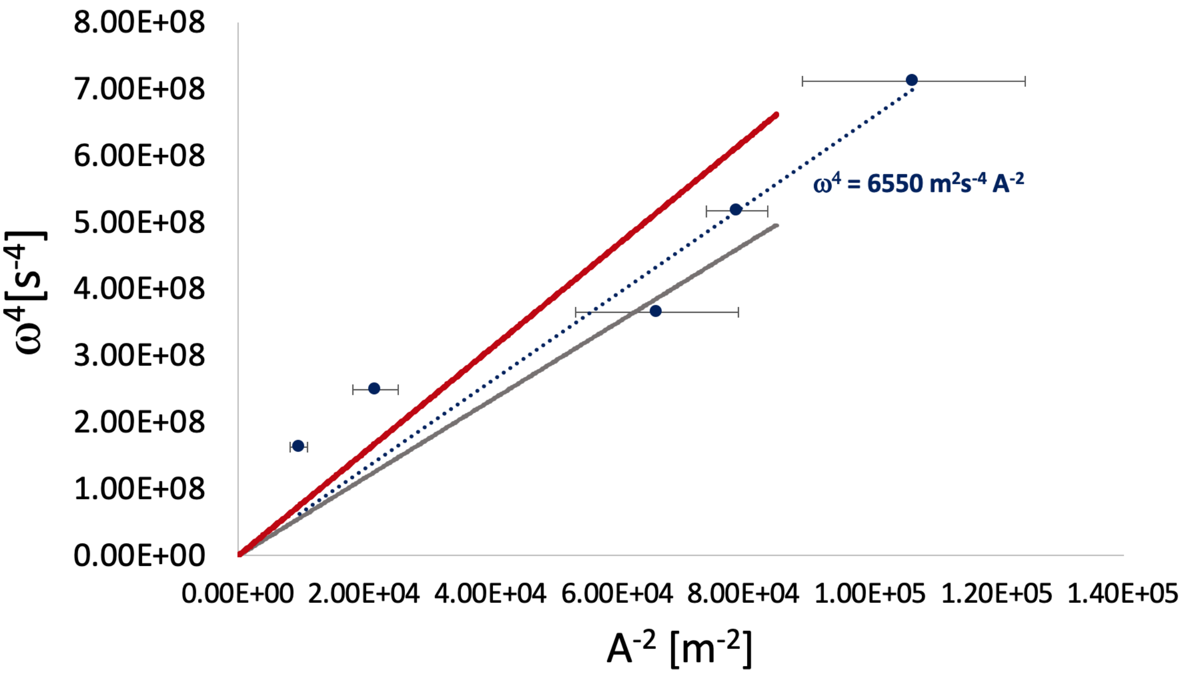

Figure 6: Diagram of the critical amplitude. For a fixed depth of 39.1 centimetres, this diagram shows the amplitude for stationary bubbles at a given frequency. The dotted line is a fitted linear function forced through the origin. The error bars represent statistical errors and the red and green lines are theoretical values with a compressibility factor (see equation II.5) $\gamma = 1.6$ for the upper line and $\gamma = 1.2$ for the lower line.

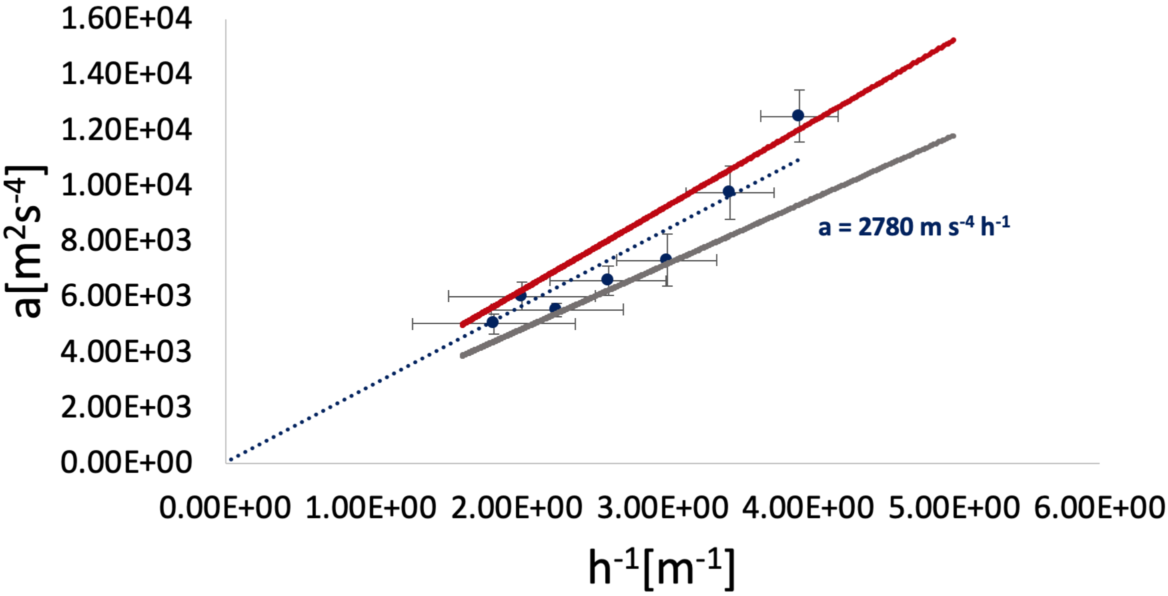

Figure 7: Variation of depth. Many diagrams analog to Figure 6 have been made for different depth of the bubbles. The slope a of those functions has been plotted as a function of the depth's inverse to validate equation II.9. The blue dots represent the experiments while the red and grey lines represent the theoretical values. The obtained values for the compressibility factor (see equation II.5) are $\gamma = 1.6$ for the upper limit (red line) and $\gamma = 1.2$ for the lower limit (grey line). The dotted line is the regression.

IV.2 Discussion

While doing the first measurements, I rapidly attained the shaker's limits. That means there was only a defined range of frequency in which I could measure. A low frequency speaks for a high amplitude and vice-versa. In both cases the power of the oscillator came to be insufficient. Close to the borders the measurements started to get complicated which explains the points of lower accuracy for the two highest amplitudes in Figure 6. To optimise the range of measurements I decided to increase the bubbles' depth by using longer tubes. By doing that, the system got more stable, which had a positive repercussion on the data. The next issue I would then encounter is the mass of the column that would lower the stability of the set up. All in all, I was able to go around the problem and enlarge the range of measurements using longer tubes.

As the fitted line in Figure 7 lays in between the calculated limits we can say that the compressibility factor γ equals to

$$\gamma = 1.4 \pm 0.2 \quad .$$

This speaks for an adiabatic compressibility as assumed in the theory.

Overall, one can conclude that equation II.9 gives an accurate result to the state of the bubble.

V Dynamics in a Water Column

V.1 Experimental Results

In this section, the orange points on the diagrams represent the experimental values whereas the blue line is a simulation following the equation II.10. The simulations were run with the software *Mathematica*. Note that the frequency used for all experiments in this section is $\omega = 24\,\mathrm{Hz}$ and the drag coefficient was kept constant, $C = 0.47$.

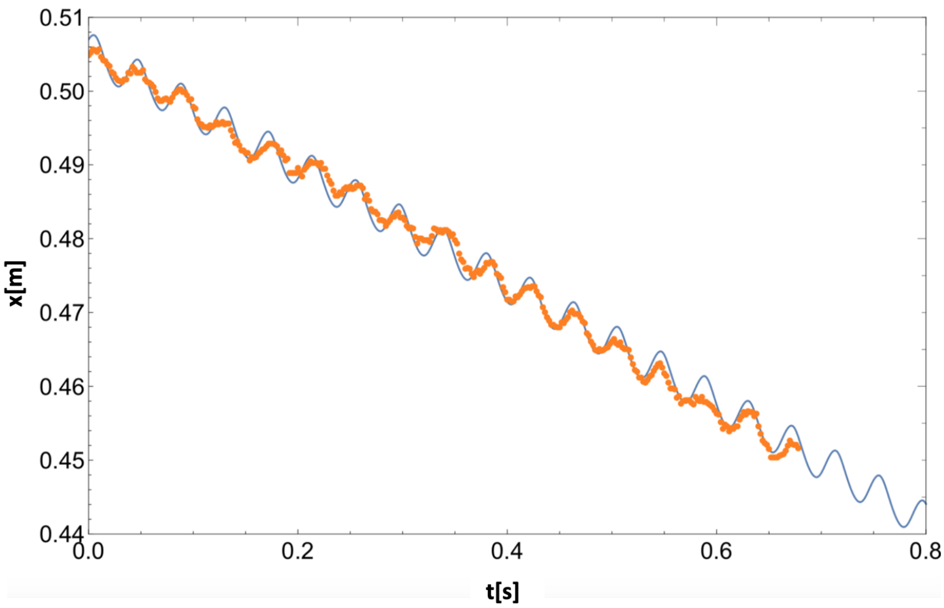

Figure 8: Motion of a rising bubble of radius $r = 0.38\,\mathrm{mm}$ in a vertically oscillating column of water. The amplitude chosen for this motion was $A = 2.46\,\mathrm{mm}$.

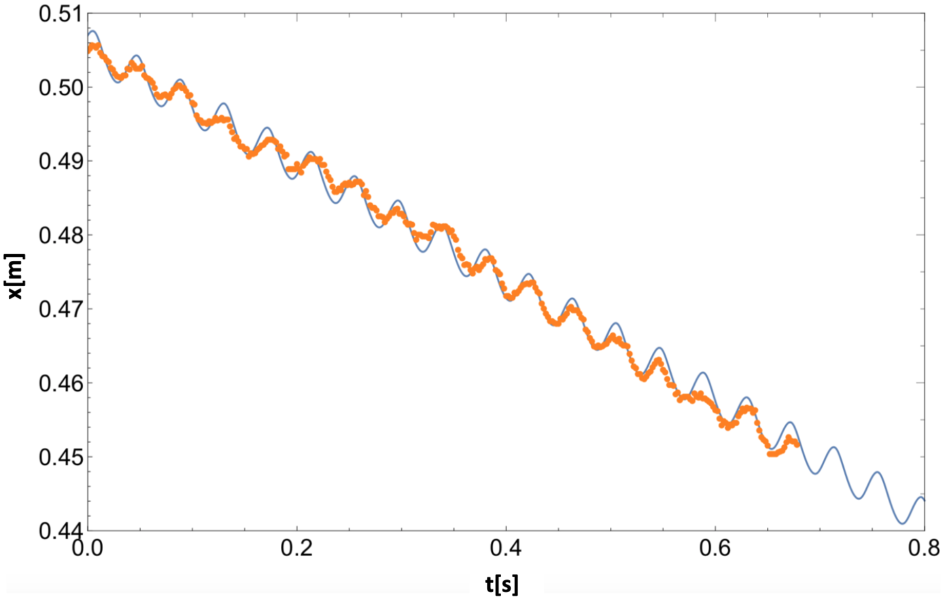

Figure 9: Motion of a rising bubble of radius $r = 0.63\,\mathrm{mm}$ in a vertically oscillating column of water. The amplitude chosen for this motion was $A = 1.96\,\mathrm{mm}$.

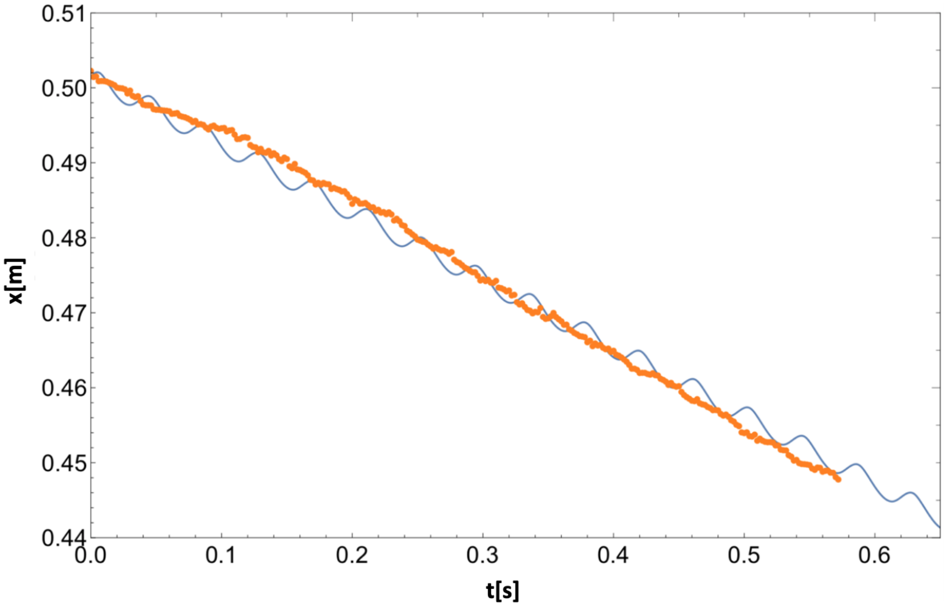

Figure 10: Motion of a rising bubble of radius $r = 0.43\,\mathrm{mm}$ in a vertically oscillating column of water. The amplitude chosen for this motion was $A = 1.03\,\mathrm{mm}$. The coefficient of added mass was reduced by 33 %.

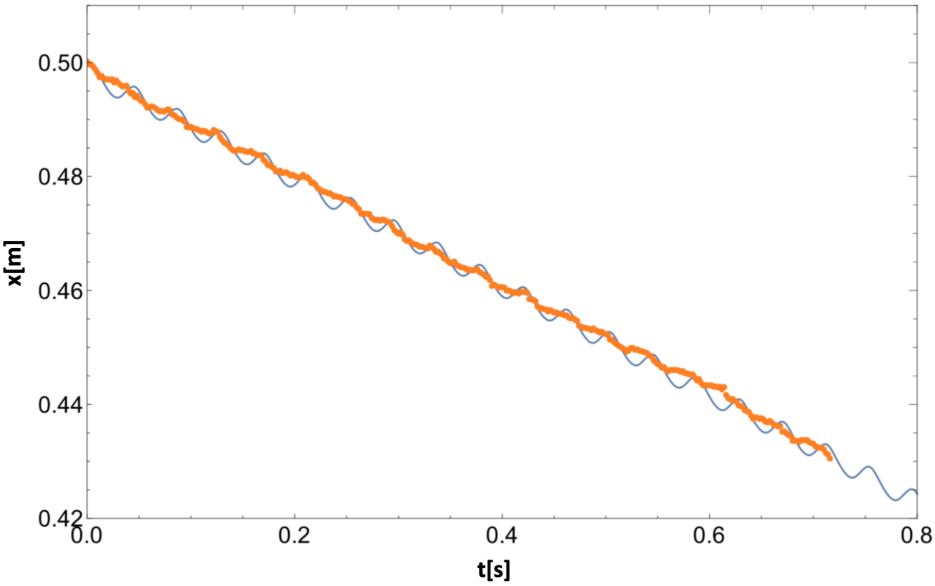

Figure 11: Motion of a rising bubble of radius $r = 0.63\,\mathrm{mm}$ in a vertically oscillating column of water. The amplitude chosen for this motion was $A = 1.26\,\mathrm{mm}$. The coefficient of added mass was reduced by 33%.

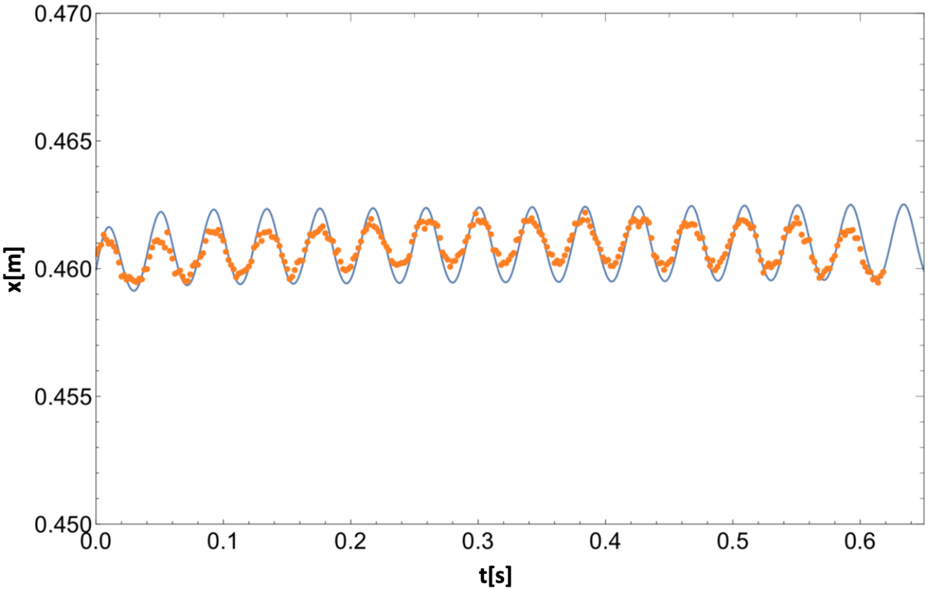

Figure 12: This diagram shows the development over time of a sinking air bubble in water ($r = 0.3\,\mathrm{mm}$). The calculated Reynolds number for this motion is $Re = 1.9$. The measured amplitude of the oscillator was $A = 3.4\,\mathrm{mm}$.

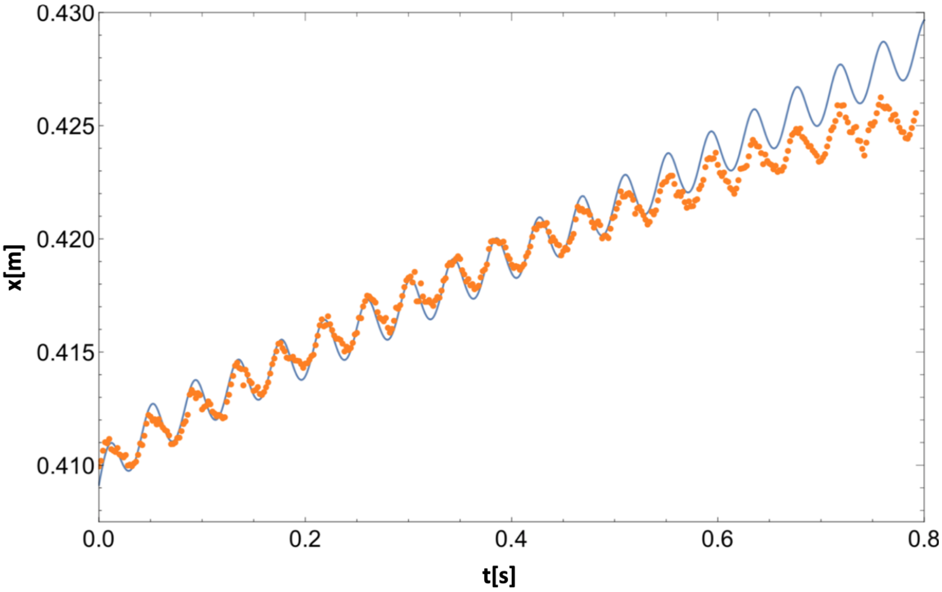

Figure 13: This diagram shows the development over time of a sinking air bubble in water($r = 0.4\,\mathrm{mm}$). The calculated Reynolds number for this motion is $Re = 16$. The measured amplitude of the oscillator was $A = 4.2\,\mathrm{mm}$.

V.2 Discussion

One can see for the rising bubbles in water, that the simulation predicts significantly higher amplitudes than the ones that have been experimentally observed whenever the system was oscillated with a small amplitude (see Figures 10 and 11). The bigger the amplitude the more added mass there is and vice-versa. If the added mass is small, there is less damping and the simulation will predict bigger amplitudes. A larger amplitude leads to a more significant the change in volume. This implies a greater amount of water oscillating around the bubble so more added mass. As one decreases the amplitude, the opposite happens. All together, it is problematic to predict the bubble's motion in a case of low amplitude with the equation II.10. One can either adapt the coefficient of added mass to make the average time of sinking between the simulation and the experiment equal (as done in Figures 10 and 11). Another possibility is to meet the amplitude given by the experimental data on Figure 11 by decreasing drastically the coefficient of added mass to match the experiments' amplitude, in what case the bubble will rise clearly faster.

All in all, if one must decrease the added mass in the simulation to make the average time of rising fit reality, the simulation will predict greater amplitudes since the damping will have been decreased. In cases of small amplitudes, it is not reasonable to describe the motion of rising bubbles using equation II.10.

Comparing Figures 12 and 13 one can see differences in the bubble's radius and the amplitude. What was concluded looking at all the results, is that the motion of bubbles of smaller radii can be more accurately described than the others. This is qualitatively explained in section II.2. Regarding the amplitude, for sinking bubbles small amplitudes are favoured since the bubbles' speed is then lower.

After studying the results, the observation was made that a "calmer" system was recommended. The idea became to find something comparable to a scale of stability. The Reynolds number of the motions was then calculated and it appeared to be a good indicator since cases of small Reynolds numbers were described more precisely than other cases.

The challenge in the measurements of the motion was to obtain a bubble of small radius, isolated from others.

VI Dynamics in an Oil Column

VI.1 Experimental Results

In this section, the orange points on the diagrams represent the experimental values whereas the blue line is a simulation following the equation II.13. The simulations were run with the software Mathematica. The frequency is kept constant, $f = 20\,\mathrm{Hz}$, and the oil used was sunflower oil (see appendix).

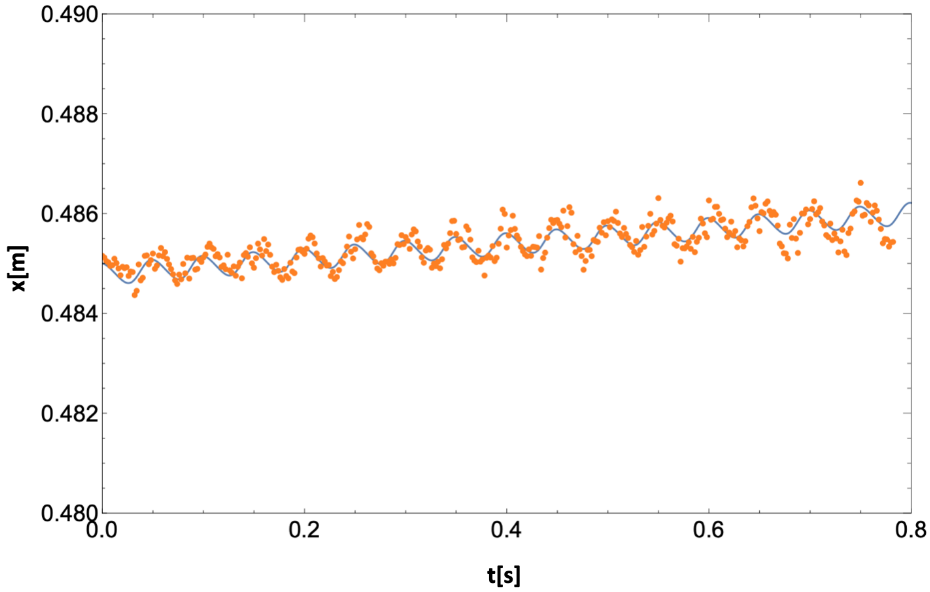

Figure 14: This diagram shows the development over time of a sinking air bubble, $r = 0.4\,\mathrm{mm}$, in oil. The calculated Reynolds number for this motion is $Re = 0.02$. The amplitude of the oscillator is $A = 6.2\mathrm{mm}$.

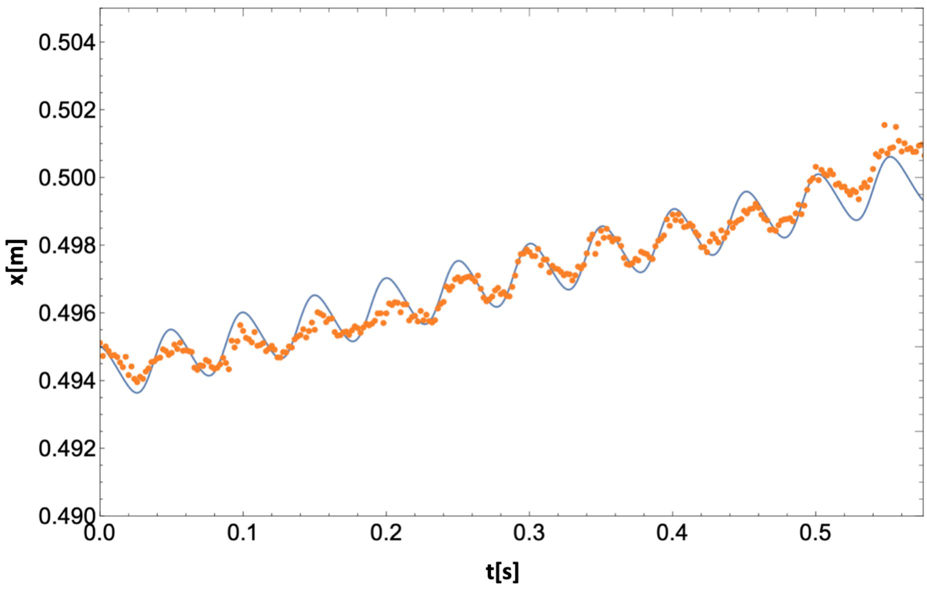

Figure 15: This diagram shows the development over time of a sinking air bubble, $r = 0.7\,\mathrm{mm}$, in oil. The calculated Reynolds number for this motion is $Re = 0.25$. The amplitude of the oscillator is $A = 7$ mm.

VI.2 Discussion

It is visible that the fit on Figure 14 is more exact than the one in Figure 15. This can be explained using the same principles as the ones interpreting Figures 12 and 13 (see section V.2), a small radius, a small amplitude and thereby a small Reynolds number bring stability to the system. Looking at the Reynolds numbers calculated for the motions in oil, one can use Stokes' law. This treat gives larger borders to the accuracy of the model. One can see that even though smaller amplitudes imply more precision, it is possible to describe accurately motions in oil that experience a rather big amplitude comparing to the ones in the previous section. All together, one can say that the range of accurateness of the simulation in oil is greater than the one in water.

The motion's flow being more stable the oscillation around the bubble is less significant. It can therefore be neglected. Flowingly, the added mass can be removed from the equation of motion, which takes away many insecurities. Equation II.13 that has been used to describe sinking bubbles in oil relays on easier physics one knows how to master. It is as well visible in oil, comparing Figures 14 and 15, that a low Reynolds number speaks for more exactitude. The idea was to pick a liquid that is viscous enough to get a more stable flow and use Stokes' law. I believe that in other liquids fulfilling the previous condition, an accurate simulation of a bubble's motion could be achieved with the same equation.

To conclude, one can see in subsection VI.1 that the equation II.13 is accurate for the description of sinking bubbles in oil.

VII Range of Accuracy of the Dynamic Model

A key point to obtain a working simulation is to have a stable system. Like that, the bubbles will move in a more predictable way. A good measure for the stability of system is the Reynolds number. The lower the value the higher the stability. The first factor that one can change to alter the Reynolds number is the velocity. As the velocity is proportional to the Reynolds number, one will target low velocities. In addition, if a sinking bubble has a high acceleration, it will move with a high velocity and its added mass will be greater, leading to a less predictable system. Choosing a low radius of the bubble (see Figures 12 and 13 and Figures 14 and 15) reduces the bubble's velocity. Tending towards smaller amplitudes by increasing the frequency and / or the bubble's depth shows to be an efficient and optimal choice as well to make the sinking bubbles move slower. If the simulation of rising bubbles is carried out in water it is recommended to avoid too small amplitudes as explained in section V.2.

The second factor that helps gaining stability in the system is the viscosity of the liquid as shown in equation II.14. I switched liquids from water to oil which allowed me to use equation II.13. It is convenient to do so since a major issue of the equation II.10 is the added mass. As previously shown, the coefficient of added mass is dependent on the shape of the bubble which is generally unpredictable. The fact that the added mass is eliminated in equation II.13 offers a broader range of accuracy of the simulation.

VIII Conclusion

The major part of the work that has been done in this paper was to experimentally confirm equations II.9 and II.10. As I am the first one to do this, one can for the first time know how to reach sinking bubbles, by what means and approximately in what cases one can use the equations to describe the bubble's motion.

Even though I got confronted pretty quickly by the oscillator's limits, equation II.9 seemed to work fairly well. Provided that the experimental values match the theoretical ones, I concluded that this description was accurate.

I have investigated more thoroughly the dynamic behaviour of the bubble, since it is the one that covered the most insecurities. After reading this paper, one should be able to understand where the limits of the given equations are and why they even exist.

As the range of use of equation II.10 got shortened over and over, I wanted to be able to simulate accurately a wider range of motions, I chose to investigate a system that was more stable than the one in water and I experimented in Oil. The new theory in the second part of section II.2, revealed being very satisfying as it matched well the measurements. Moreover, it uses simpler physics (see equation II.13), which offers a broad accessibility to the understanding of the non-trivial phenomenon of sinking bubbles.

A Measurements of Sunflower Oil's Viscosity

To measure the viscosity of a liquid you can simply let an object fall in the liquid and apply the following equation:

$$F_G = F_F + F_B$$

$$mg = 6\pi\eta\dot{x}r + \rho g V$$

$$\eta = g\,\frac{m - \rho V}{6\pi\dot{x}r} \tag{A.15}$$

Figure 16: This picture shows the set up of the viscosity measurements, consisting in letting a sphere fall in the liquid and track its motion to get the velocity of the sinking object.

All the parameters were then entered in equation A.15 and my result for η was:

$$\eta = 0.000073 \pm 0.000005\ \frac{\text{kg m}}{\text{s}} \quad .$$

Note that the measurements were made at room temperature.

B Calculation of the Capillary Length

$$\frac{r}{\lambda_{cap}} = \sqrt{\frac{\rho g r^2}{\sigma}}$$

The variable ρ stands for the liquid's density, g is the earth's acceleration, r the bubble's radius and σ the surface tension of the liquid. In the calculations I used the following values:

$g = 9.81\frac{\text{m}}{\text{s}^2}$

$\rho_w = 0.997\frac{\text{kg}}{\text{m}^3}$

$\sigma_w = 72 \times 10^{-3}\frac{\text{N}}{\text{m}}$

$\rho_{oil} = 0.895\frac{\text{kg}}{\text{m}^3}$

$\sigma_{oil} = 33.5 \times 10^{-3}\frac{\text{N}}{\text{m}}$

Calculations for water:

- $r = 3mm$

$$\frac{r}{\lambda_{cap}} = \sqrt{\frac{0.997\frac{\text{kg}}{\text{m}^3}9.81\frac{\text{m}}{\text{s}^2}0.003^2\text{m}^2}{72 \times 10^{-3}\frac{\text{N}}{\text{m}}}} = 0.11$$

- $r = 7mm$

$$\frac{r}{\lambda_{cap}} = \sqrt{\frac{0.997\frac{\text{kg}}{\text{m}^3}9.81\frac{\text{m}}{\text{s}^2}0.007^2\text{m}^2}{72 \times 10^{-3}\frac{\text{N}}{\text{m}}}} = 0.26$$

Comparing the results it is noticed that the ratio of the radius to the capillary length is much larger for bubbles of radius 7mm. This means that the approximation of their shape to a sphere is not fully right. Hence, a better approximation is achieved choosing bubbles of smaller radii.

Calculations for oil:

- $r = 3mm$

$$\frac{r}{\lambda_{cap}} = \sqrt{\frac{0.895\frac{\mathrm{kg}}{\mathrm{m}^3}9.81\frac{\mathrm{m}}{\mathrm{s}^2}0.003^2\mathrm{m}^2}{33.5\times10^{-3}\frac{\mathrm{N}}{\mathrm{m}}}} = 0.049$$

- $r = 7mm$

$$\frac{r}{\lambda_{cap}} = \sqrt{\frac{0.895\frac{\mathrm{kg}}{\mathrm{m}^3}9.81\frac{\mathrm{m}}{\mathrm{s}^2}0.007^2\mathrm{m}^2}{33.5\times10^{-3}\frac{\mathrm{N}}{\mathrm{m}}}} = 0.11$$

From the calculations it is obvious that the bubbles have a much more spherical shape in oil than in water.

C Diagrams to the Static Case

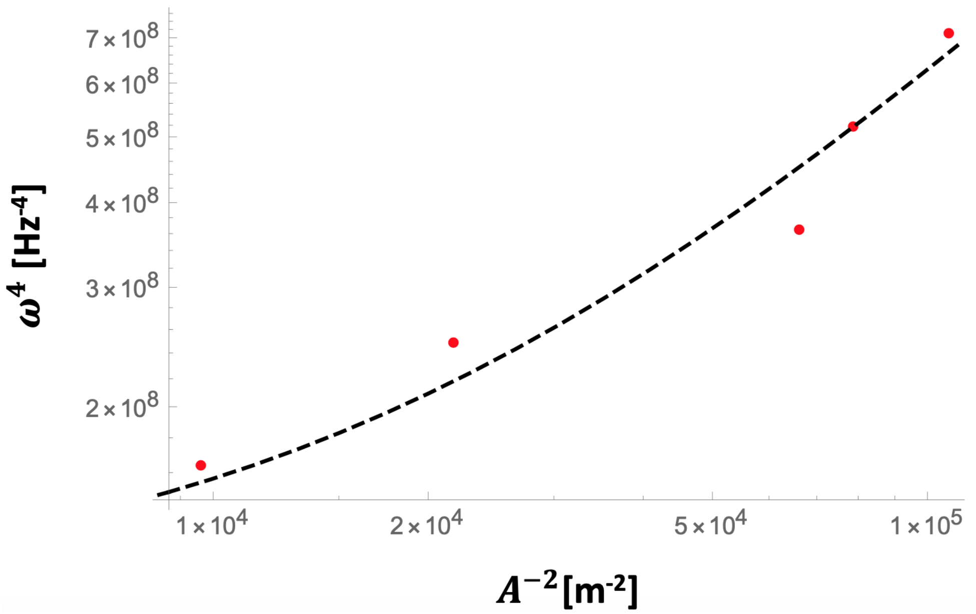

Figure 17: Logarithmic scaling of Figure 6.

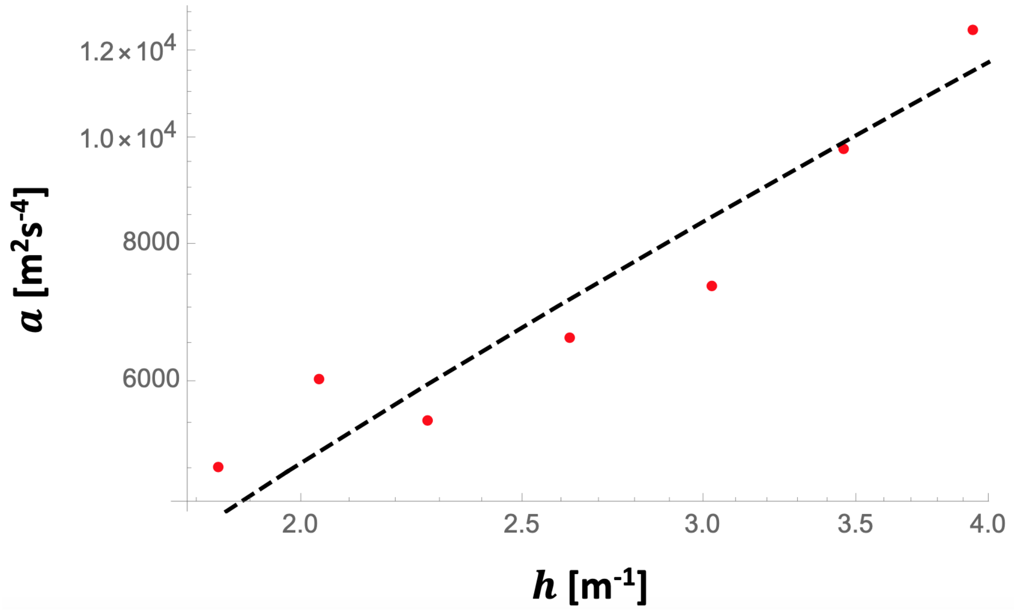

Figure 18: Logarithmic scaling of Figure 7.

Acknowledgments

I truly thank Daniel Weiss, my expert, who directed me towards the end of the project by pointing out new theoretical elements confirming my assumptions and findings and my supervisor Daniel Keller who guided me throughout the whole project, as well as Eric Schertenleib who was always of valuable advice. I also thank my friends, who were there to give me a hand whenever I needed it, and lastly, I want to thank my family who supported me throughout.

References

[1] A.H. Techet by TA B. P. Epps. 2.016 Hydrodynamics http://web.mit.edu/2.016/www/handouts/Added_Mass_Derivation_050916.pdf (visited last on August 29^{th}, 2019)

[2] Christian Gentry, James Greenberg, Xi Ran Wang, Nick Kearns. Sinking Bubble in Vibrating Tanks

[3] Eliezer, Rubin. Behavior of Gas Bubble in Vertically Vibrating Liquid Columns. *The Canadian Journal of Chemical Engineering.* 1967.

[4] Gennes, Pierre-Gilles / Brochard-Wyart, Françoise / Quéré, David. Capillarity and Wetting Phenomena, 2004. New York: Springer-Verlag.

[5] Martin Devaud, Thierry Hocquet, Jean-Claude Bacri, Valentin Leroy. The Minnaert bubble: a new approach. 2007. hal-00145867

[6] Schlichting, Hermann / Gersten, Klaus (2006): Grenzschicht-Theorie. 10. Berlin Heidelberg: Springer-Verlag.

[7] Sorokin, Vladislav & I. Blekhman, I & B. Vasilkov, VB. Motion of a gas bubble in fluid under vibration. *Nonlinear Dynamics* 2012; 67(1):147-58.